

2024-08-02

X-ray segmentation and implant design using panoramic and tangential views

Y. Xing, P. Liao, R.A. Alasleh, V. Khampatee, F. Alizadeh-shabdiz. 2024. "X-ray segmentation and implant design using panoramic and tangential views" Proceedings of the 2024 7th International Conference on Machine Learning and Machine Intelligence (MLMI), pp.260-265. <https://doi.org/10.1145/36https://hdl.handle.net/2144/50296>

"Downloaded from OpenBU. Boston University's institutional repository."

Submission Template for ACM Papers

X-ray segmentation and implant design using panoramic and tangential views

Yang Xing

Computer Science Department, Boston University Metropolitan College, yangx9@bu

Peixi, Liao

Department of Restorative Sciences and Biomaterials, Boston University Henry M Goldman School of Dental Medicine, liaopx@bu.edu

Reem AwdhE Alasleh

Department of Restorative Sciences and Biomaterials, Boston University Henry M Goldman School of Dental Medicine, alsalehr@bu.edu

Vissuta Khampatee

Department of Restorative Sciences and Biomaterials, Boston University Henry M Goldman School of Dental Medicine, vissutak@bu.edu

Farshid Alizadeh-Shabdiz

Computer Science Department, Boston University Metropolitan College, alizadeh@bu

In dental diagnostics and implant restoration planning, panoramic radiographs are crucial tools but require meticulous and time-consuming analysis due to image variability. This paper introduces an AI-based deep learning solution designed to accelerate and improve the accuracy of implant positioning by processing both panoramic and tangential images. The methodology involves developing a CNN model based on ResUNet for segmenting teeth, restorations, and other oral structures, which then forms the basis for calculating the main axes and precise locations of implants. The model autonomously suggests precise implant placement locations using PCA and linear regression, streamlining the diagnostic and planning phases. The performance of the model is evaluated using Intersection over Union (IoU) and pixel accuracy metrics, achieving an accuracy rate of 0.9785 and an IoU of 0.8483 on a dataset of images from 100 patients. The precision of implant placement is assessed by calculating distances and angles relative to actual implant locations, with predicted implant locations showing an average deviation of 0.360 mm and a maximum deviation of 0.795 mm from placements done by dental professionals. This integrated approach significantly enhances efficiency and accuracy in dental care by providing a comprehensive, end-to-end solution for implant restoration planning.

CCS CONCEPTS • \begin{CCSXML}

<ccs2012>

```
<concept>
  <concept_id>10010147.10010178.10010224.10010245.10010247</concept_id>
  <concept_desc>Computing methodologies~Image segmentation</concept_desc>
  <concept_significance>500</concept_significance>
</concept>
</ccs2012>
\end{CCSXML}
```

```
\ccsdesc[500]{Computing methodologies~Image segmentation}
```

Additional Keywords and Phrases: Image Segmentation, Dental X-ray, Teeth Segmentation, Dental Implant Planning

1 INTRODUCTION

In dentistry, X-ray images, also called radiographic images, are fundamental data sources to help dentists to make diagnoses. [1] Panoramic radiographs are filmed from extra-oral examinations where patients need to stand between the film machine and the source of the X-rays. Panoramic radiograph as a diagnostic image often used in dentistry plays an important role in providing a broad and comprehensive view of the entire oral and maxillofacial region, including the teeth, jaws, sinus, bone, and other components. However, detecting and extracting information about each tooth often requires a detailed diagnosis and extensive clinical experience. The development of automated diagnosis tools has faced many challenges such as the variation of situations of patients, and lack of clarity in images, and noises. With the development of neural networks or deep-learning models and their application, deep learning-based methods have been put forward for the purpose of helping dentists interpret radiographs and make quick diagnoses as advisory opinions for final diagnoses. One application scenario is using segmentation methods to partition the panoramic image into different regions or categories (such as tooth, sinus, and bone) so that the interpretation of each category is relatively easy for dentists.

The application of the deep learning method in dentistry has raised attention in the last five years. With the development of several popular architectures of CNN, such as UNET and other CNN models, much research with different models and different tasks (including detecting missing teeth, oral implant logical tasks, and tooth region detection) has been conducted. Typically, two types of radiograph images are used, panoramic images and CBCT images.

Before deep learning was applied to analyze oral images, some expert systems were used which were proved very biased when dealing with large datasets where variations increase. [2] Since the effectiveness of deep learning has been observed, several different networks have been employed in real life and numerous research have been conducted. CBCT images, also known as Cone Beam Computed Tomography, are a 3D imaging technique. It can capture several 2D images from different angles and then transfer these images to a 3D

volumetric dataset. Reference [3] used CBCT images and developed the TSegNet architecture for tooth segmentation based on that. Reference [4] built a process to segment teeth out by extracting feature points first. 3D modeling requires not only extra careful examination to ensure precision, but also more computational complexity which could be time-consuming. Considering the complexity of using 3D images, it is more efficient and practical to analyze 2D images such as panoramic images than 3D images. Therefore, this paper also focused on 2D oral radiographs. As for the panoramic images, Reference [5] has used VGG-16 for tooth segmentation for tooth images. Reference [6] has conducted research on how to apply U-Net family CNN on panoramic radiographs generally.

Reference [7] used Patch-FCN training tooth identification and missing region detection on an oral panoramic image. Some problems are observed that, when the dataset is small, it makes the model's performance worse in lack of generality. The unclear behavior of deep learning architectures requires the evaluation of models using additional test datasets to prevent any chance that the good performance is because of the data memory. Several models with modifications are applied for the segmentation task. Reference [8] developed a two-stage attention CNN network, where the first stage is predicting an attention map and the second stage uses U-net to do the segmentation and identification. Other architectures used in tooth segmentation include PANnet, PatchFCN, and mask RCN. ([9], [10], [11]). Besides applying different deep learning models on segmentation or object detection on radiographs, there are only a few articles focused on the application of how to make use of the output of the deep learning models, especially on implant planning. Reference [19] used an instance segmentation model to segment each tooth and label them with numbers to detect any missing tooth regions. However, the performance may suffer from unexpected situations from patients such as the overlapping of two teeth, or implanted restorations. Reference [20] put forward a dataset targeting patients who need implant operations but only the segmentation task is performed. Reference [21] used object detection methods to detect the missing tooth. The performance is good, but no implant is suggested based on the model. Reference [22] put forward an approach based on CBCT images for implant planning. Above all, the potential of using panoramic images for implant planning based on deep learning models is still there to be developed.

2 DATASET

The research focuses on 2D oral radiographs. The source of the training and testing set is panoramic images, which are fundamental oral images that help identify pathological structure, make a diagnosis, and decide treatment plan. The panoramic x-ray produces a flat image of the curved structure. It usually provides details of the bones and teeth. In the first part of this research, the purpose of building a CNN model is to segment the panoramic image into six parts, Sinus, Tooth, Restoration, Bone, Root Canal, and Major Nerve. An example is shown in Figure. 1.

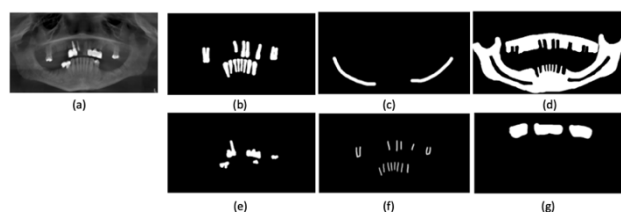


Figure 1: An example of panoramic images and six segmentations: (a)panoramic radiograph,(b)teeth,(c)major nerve,(d)bone,(e)restoration,(f)root canal,(g)sinus

Besides the panoramic images, another angle of the whole oral image (Tangential radiograph) is also added as the input to the machine learning model which can be taken from the patient's cheek. A tangential radiography image refers to an X-ray image of a tooth that is taken from a tangential or oblique angle, rather than a direct, frontal view. This angle allows for the visualization of specific aspects of a tooth that may not be visible in a standard, straight-on X-ray image. An example is shown in Figure. 2. Tangential images share the same six structures as the output that need to be segmented out, which are Sinus, Tooth, Restoration, Bone, Root Canal, and Major Nerve. By adding the tangential image to the dataset, the model can better recognize different structures in the oral since panoramic and tangential images share some similarities.

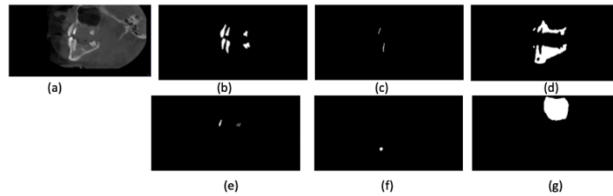


Figure 2: An example of tangential images and six segmentations: (a)panoramic radiograph,(b)teeth,(c)major nerve,(d)bone,(e)restoration,(f)root canal,(g)sinus

The dataset is annotated by experienced dentists from Boston University dental school. Each patient will have two radiographs including a panoramic and a tangential view. Dentists annotate six segments on each radiograph, which are tooth, sinus, restoration, nerve, bone, and root canal. The total number of patients is 100, which means there are a total of 100 panoramic images, denoted as P00 ~ P99, and 100 tangential images, denoted as T00 ~ T99.

The dataset is split into two datasets where the first dataset is used to train and test the first stage of the model the second dataset is used to evaluate the whole performance of the model and the second dataset is used to evaluate the whole performance of the model.

The first dataset consists of 100 patients each having one panoramic radiograph and one tangential radiograph. The detailed experiment settings for pursuing a higher performance of the first stage's task, which is the segmentation of the 2D images will be discussed below. Two different ways to shape the dataset have been considered. The first method assumes the panoramic image of a patient can also assist in increasing the accuracy of the segmentation of the tangential image, (and vice versa). In this case, both panoramic and tangential images are combined as one input and both of the images get segmented together. In that case, both tangential and panoramic images for the same patient will be taken as one data sample. The total input dataset size would be (100, 512, 512, 2), where 100 is the number of patients, 512*512 is the size of one image, and 2 means both panoramic and tangential images. For example (33, 512, 512, 0) means the panoramic image of patient 33. The second method takes each tangential and panoramic image as an independent input to the model. In this case, the total input dataset size would be (200, 512, 512, 1) and the output dataset size would be (200, 512, 512, 6).

The second dataset consists of 20 patients each has one panoramic radiograph. For each patient in the second dataset, the dentists will suggest an implant with the appropriate for each region of a missing tooth. The actual

implant planned by professionals will be used as the truth when compared with the predicted implant from the output of the model.

3 MODEL

3.1 Architecture

The model consists of two stages where the first stage is to train a CNN from 100 panoramic images and tangential images to identify and segment different structures from the oral image and the second stage is to use the pre-trained CNN to provide tooth and restoration segmentations, apply post-processing methods on that to help divide every tooth one by one and locate on the missing tooth, and use PCA to locate the main axes of two adjacent tooth near the missing tooth, and use Linear Regression to calculate the main axes of the missing tooth. A detailed architecture is provided in Figure 3.

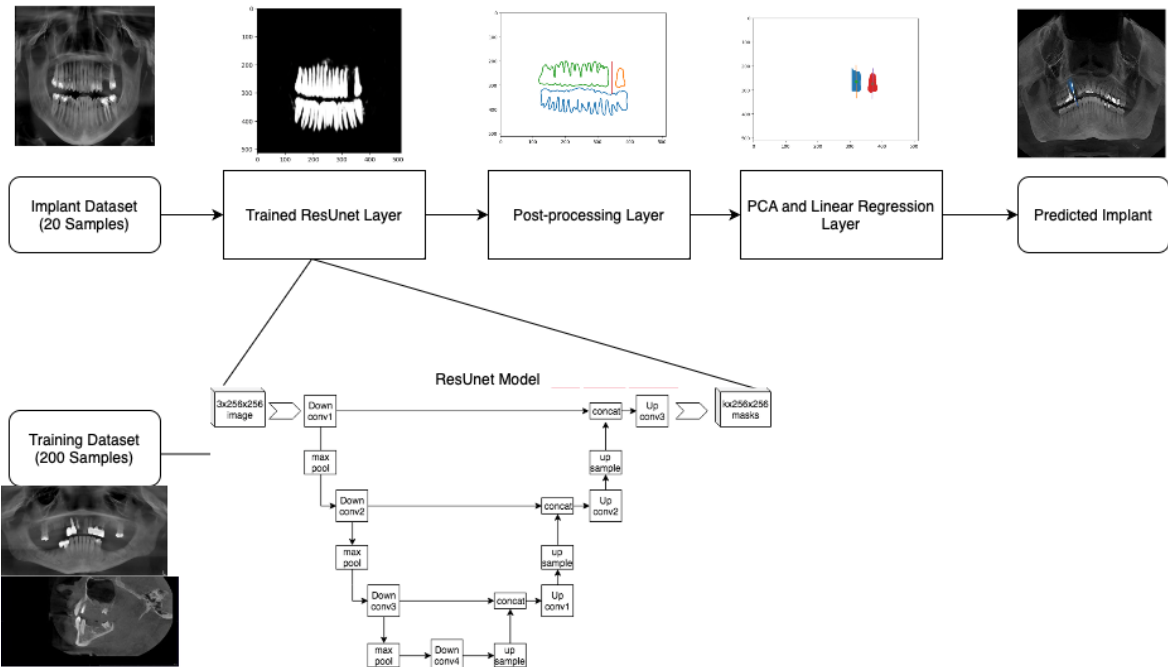


Figure 3: The architecture of the model

3.2 Segmentation Model

Two typical convolutional neural network architectures are adopted for the 2D images: U-Net and ResUnet. U-Net was developed for biomedical image segmentation and belongs to the convolutional neural network family, [13]. One advantage of U-net is having a relatively higher performance especially when there are fewer training images. Another advantage is its lightweight architecture, which makes the computation and training process very fast. U-net has become popular in the training segmentation of medical images because of its good performance. Reference [14] notes that half of the essays that train oral images using CNN use U-net-related

networks. ResUNet is a more modified architecture by combines the idea of residual networks and Unet. This combination makes ResUNet particularly powerful for semantic segmentation tasks in medical imaging, satellite image analysis, and various other fields where precise object delineation is essential. Note that adding more residual blocks means more skip connections, which may lead to a problem of overfitting. This is an important issue, since the number of samples in the training set is not large, only one hundred samples. In order to avoid this issue the dropout method is adopted at each layer which will randomly remove a certain portion of neurons. In this analysis, both ResUNet and ResUNet-with-dropout have been considered and assessed.

As for the loss functions, the most common loss functions that are used in medical segmentation tasks are cross entropy and dice loss, [16]. Cross entropy (CE) measures dissimilarity between the two different distributions, the prediction and the ground truth. For a CNN-based segmentation task, the cross-entropy loss is defined by

$$L_{CE} = -\frac{1}{N} \sum_{c=1}^C \sum_{i=1}^N g_i^c \log s_i^c,$$

where g_i^c is the ground truth binary indicator of class label c of voxel i , and s_i^c is the corresponding predicted segmentation probability. Another loss function is Dice loss. Dice loss can directly optimize the Dice Similarity Coefficient (DSC) which is the most used segmentation evaluation metric. Unlike weighted cross entropy, Dice loss does not require class re-weighting for imbalanced segmentation tasks. It is defined by

$$L_{Dice} = 1 - \frac{\sum_{c=1}^C \sum_{i=1}^N g_i^c s_i^c}{\sum_{c=1}^C \sum_{i=1}^N (g_i^c + s_i^c - g_i^c s_i^c)},$$

where g_i^c is the ground truth binary indicator of class label c of voxel i , and s_i^c is the corresponding predicted segmentation probability. The compound loss is the (weighted) combination of the above loss functions. It is defined by,

$$L_{DiceCE} = L_{CE} + L_{Dice}.$$

Dice loss is proven to have good performance when detecting edges [15]. Using compound loss can combine the advantages of both two good loss functions. All these loss functions will be used as candidate loss functions to improve the model performance. The model is trained with different combinations of loss functions and data inputs and uses Adam as the optimizer. IoU is used as a measure of the accuracy of the model. Different approaches for data enhancements are used. The data augmentation techniques used in the model include random rotation, flips, translations, and adjusting brightness. Normalization is also needed to scale the value of each pixel from [0,256] to [0,1]. Some other standard preprocessing processes such as CLAHE, which is put forward by [12], are also included. Contrast-limited adaptive histogram equalization (CLAHE) is a technique for increasing the visibility of a foggy image or video. It operates by dividing an image into small, non-overlapping regions, often referred to as "tiles" or "patches," and then applies histogram equalization independently to each of these regions.

3.3 Post Processing

Once the image segmentation is done by the deep learning model, a segmented panoramic image is used in the second stage to predict the implant location. The second stage process is as follows: the first step is to locate gaps in the image that are large enough for implants, then consider adjacent teeth of the gap, where an implant is needed. Then a machine learning algorithm PCA is applied to calculate the main axes of each tooth. The implant gets positioned at the middle line of the left and the right tooth's main axes. Principal Component Analysis (PCA) is used to find the main axes of an object or in this case left and right tooth. Even though PCA

works for most cases, there are cases in the line that is not accurate enough. Therefore, the following methods are used to fine-tune the results.

In most cases, adjacent teeth are seen as connected objects, which causes an issue in calculating the main axis of adjacent teeth. In order to address this issue, the following image processing methods are used before the main axis calculation of adjacent teeth.

First, both image erosion and dilation are used to help reduce the connected teeth so that they can be easily located in connected cases as a single tooth on the left or the right side of the implant location. Image erosion is a process that reduces the size of foreground objects (usually represented as white pixels) in an image while preserving their shape. Image dilation, on the other hand, is a process that increases the size of foreground objects while preserving their shape. Both of them use a structuring element to slide over the image to calculate whether each pixel will be modified. After applying image erosion and image dilation (also called image opening), some teeth still stay connected. This may cause the main axes of the tooth to have an offset if the entire boundary is taken into consideration for PCA. To address this issue, the tooth gets divided into two parts: the root and the crown. As for connected teeth, the crown part usually can be seen as a straight line, while the roots can be seen as a curve that has many variations. Thus, the dividing points of each tooth can be found by taking the first-order derivative of the curve and finding the dividing points where the first-order derivative equals zero.

3.4 PCA and Linear Regression Predictor

Once the image segmentation is done by the deep learning model, a segmented panoramic image is used in the second stage to predict the implant location. The second stage process is as follows: the first step is to locate gaps in the image that are large enough for implants, then consider adjacent teeth of the gap, where an implant is needed. Then a machine learning algorithm PCA is applied to calculate the main axes of each tooth. The implant gets positioned at the middle line of the left and the right tooth's main axes. Principal Component Analysis (PCA) is used to find the main axes of an object or in this case left and right tooth. Even though PCA works for most cases, there are cases in the line is not accurate enough. Therefore, the following methods are used to fine-tune the results.

After the boundary of the adjacent tooth is extracted from the tooth image, using PCA to calculate the main axes of each tooth, the final step is to implement a linear regression to calculate the middle line that can divide the area between these two main axes of the tooth equally and use it as the suggested implant location.

To evaluate the correctness of the calculated implant from the algorithm, another new dataset of 23 patients is used for testing accuracy. Each prediction is compared with the implant designed by three dentists who are fully trained in dental planning.

4 EXPERIMENTS AND RESULTS

4.1 Training ResUnet model and Comparison between results

Different combinations of settings including two types of input datasets, two CNN models, and three loss functions, have been tested. Training results including IoU, Accuracy, and Loss measurements are shown in Figure. 4. A sample of a panoramic image of input data, segmentation ground truth, and prediction is shown in Figure. 5.

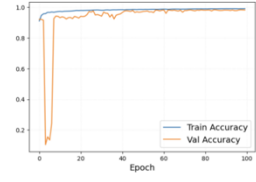
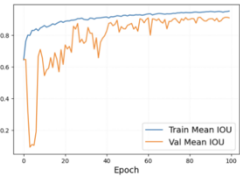
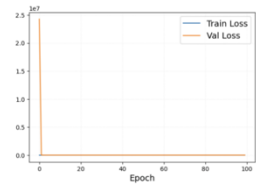


Figure 4: The history of each performance measurement among epochs in a training process

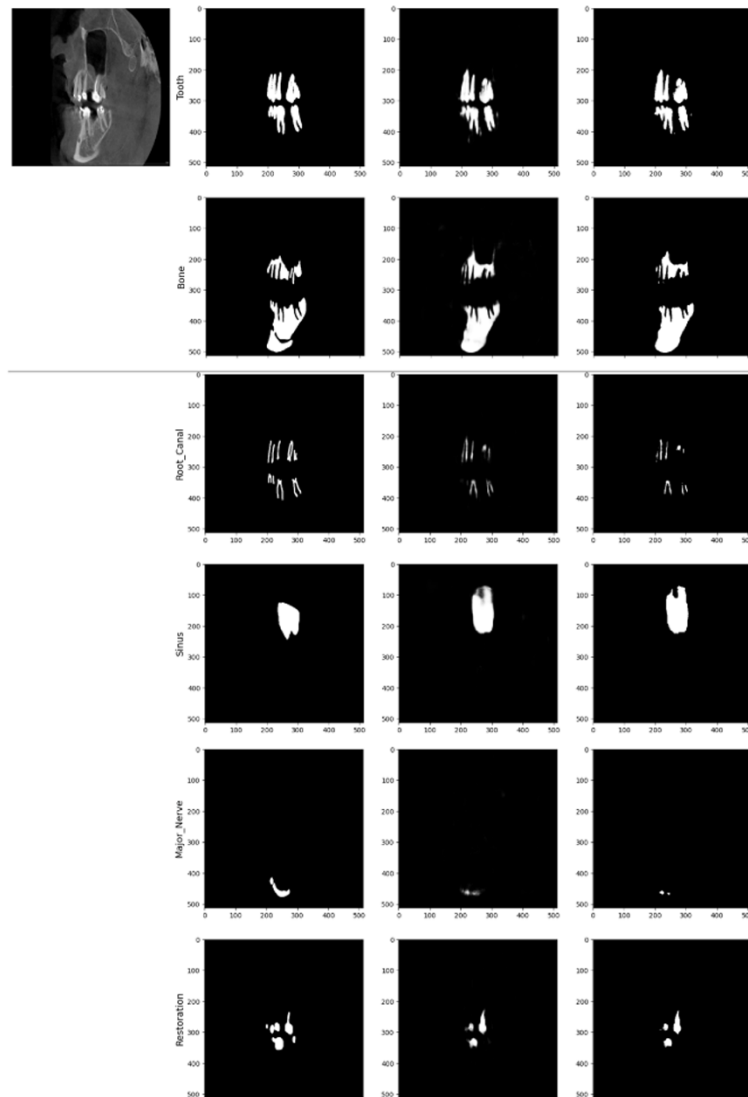


Figure 5: The architecture of the model

The performance of the model under each combination of the settings is shown in Table. 1, followed by the discussion of the comparison of each setting while controlling other hyperparameters.

Table 1: The performance measure matrix under different experiment settings

Model	Data Size	Argumentation	Loss function	Train Accuracy	Train IoU	Test Accuracy	Test IoU
ResUnet_Dropout	(100,512,512,2)	FALSE	CE	0.984	0.6694	0.9732	0.8192
ResUnet	(100,512,512,2)	FALSE	CE	0.9902	0.9103	0.973	0.8188
ResUnet_Dropout	(100,512,512,2)	FALSE	Dice	0.9929	0.903	0.9763	0.8308
ResUnet	(100,512,512,2)	FALSE	Dice	0.9904	0.8948	0.9759	0.8278
ResUnet_Dropout	(100,512,512,2)	FALSE	Dice+CE	0.9959	0.936	0.9771	0.8396
ResUnet	(100,512,512,2)	FALSE	Dice+CE	0.9959	0.9614	0.9765	0.8363
ResUnet	(200,512,512,1)	FALSE	CE	0.9883	0.8964	0.977	0.8356
ResUnet_Dropout	(200,512,512,1)	FALSE	CE	0.9942	0.9426	0.9765	0.832
ResUnet	(200,512,512,1)	FALSE	Dice	0.9889	0.888	0.9765	0.826
ResUnet_Dropout	(200,512,512,1)	FALSE	Dice	0.9885	0.8839	0.9761	0.8258
ResUnet_Dropout	(200,512,512,1)	FALSE	Dice+CE	0.9899	0.9075	0.9785	0.8483
ResUnet	(200,512,512,1)	FALSE	Dice+CE	0.9876	0.8922	0.9773	0.8448
ResUnet_Dropout	(200,512,512,1)	TRUE	CE	0.9842	0.8514	0.9728	0.7994
ResUnet	(200,512,512,1)	TRUE	CE	0.9835	0.8487	0.9718	0.7921
ResUnet_Dropout	(200,512,512,1)	TRUE	Dice	0.9834	0.8565	0.9702	0.7939
ResUnet	(200,512,512,1)	TRUE	Dice	0.9828	0.842	0.9684	0.7777
ResUnet	(200,512,512,1)	TRUE	Dice+CE	0.9902	0.9033	0.9697	0.788
ResUnet_Dropout	(200,512,512,1)	TRUE	Dice+CE	0.9912	0.9092	0.9692	0.7875

First, whether the model can improve performance by adding tangential images to the model compared with only using panoramic images was examined. Overall, using tangential and panoramic images, regardless of the way to combine them, there is a higher accuracy and IoU on both training and testing datasets. Next, the correlations between panoramic and tangential images from the same patient will also be examined. Overall, More variation is observed when choosing to stack panoramic and tangential images linearly. However, the highest accuracy and IoU on the test set are achieved by stacking panoramic and tangential images linearly instead of vertically. The overall performance of each CNN architecture is compared. Although the average accuracy and IoU seem to show no difference on the test set, a lower IoU and accuracy are observed on the training set when using the ResUnet with dropout layer architecture. Performance among different loss functions is also recorded. It is observed that cross-entropy can not detect the edges of each tooth shape very well and always have some pixels between the blank area between two adjacent teeth. So combining both dice loss and cross entropy loss is used to achieve higher performance. From the table. 1, the compound loss that combines dice and cross-entropy has the highest test IoU and accuracy.

The model that has the highest test accuracy and test IoU will be selected as the final model, which will be used in the second stage. The model setting includes the ResUnet model adding dropout layers, using linearly

stacked panoramic and tangential data, using the data argumentation process, and using compound loss as a loss function.

Considering the size of the dataset is relatively small, no transformer-based model is applied as the backbone for the first stage model. But Patch-FCN and Unet are also considered as the baseline to validate the performance of the ResUnet. The hyperparameters such as the loss functions, and the data size are kept the same for reference. The result is shown in Table 2.

Table 2: The average performance measure matrix of different models

Models	Average of Train Accuracy	Average of Train IoU	Average of Test IoU	Average of Test Accuracy
ResUnet	0.988644444	0.893011111	0.816344444	0.974011111
ResUnet_Dropout	0.98544	0.85447	0.80931	0.9721
Grand Total	0.986957895	0.872726316	0.812642105	0.973005263

4.2 Post-processing and Main Axes Implant Prediction

The next step is to use the prediction of the best model to get the segmentation of the tooth and use the predicted tooth image to make an implant plan. The prediction will be mapped back to the original X-ray image and compared with the implants planned by dentists to evaluate the performance of the whole process. The computation process of the implant planning is shown below in Figure. 6. A few samples of the final output are also shown in Fig. 7.

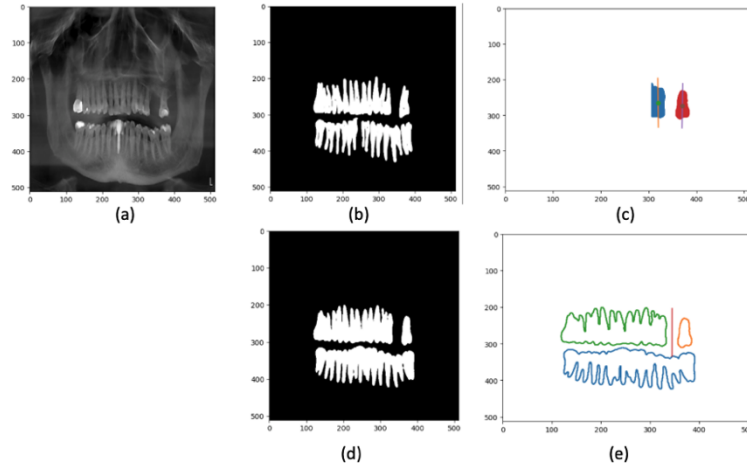


Figure 6: An example of the computation logic about predicting the implant from panoramic images: (a)panoramic radiograph,(b)teeth of the ground truth,(c)the extracted two adjacent teeth from prediction,(d)prediction of the teeth(e)calculating the main axes

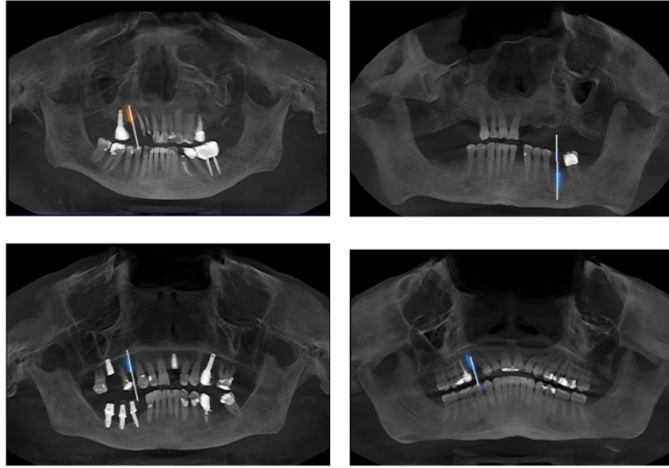


Figure 7: Samples of the comparison between the implant suggested by the dentist and by the model. The white straight line is the main axis of the implant calculated from the model and the colored implant is made by the dentist.

Since there are almost no available approaches as a benchmark for the second stage's work, we use the actual implants planned by the professionals from the dental school and analyze the result by performing a statistic test. To evaluate the correctness of the prediction made by the model, another 24 new samples (in addition to the training and the testing set) are used to go through the entire pipeline to get the output. The outputs are compared with the actual implants annotated by the dentists to compute the difference in the angle of the main axes and the difference in distance. The average difference in the angle is 2.09 degrees and the average distance between the prediction and the actual implant is 0.36mm. Since the sample size is 24, a T distribution is used to calculate the confidence interval. With a significant level of 99 percent (alpha equals 0.01), The confidence interval of the average distance between the prediction and the actual implant is [0.17mm,0.55mm]. The detailed statistics of each sample and the key statistics are shown below in Table 3.

Table 3: The evaluation of the distance and angle between the predicted implant and the actual implant

mean	std_error	freedom	Confidence_level	Confidence_Interval_lower	Confidence_Interval_upper
0.35958135	0.2225021	23	95%	0.321877652	0.397285056
0.35958135	0.2225021	23	99%	0.173802085	0.545360623

5 DISCUSSION AND CONCLUSION

Some articles focus on improving segmentation quality by improving image quality and transforming training labels. While a few articles employ multi-label methods to enhance the model's ability to recognize challenging panoramic views, only panoramic images are used in the training process. For instance, reference [17] annotates different classes of teeth and reference [18] uses a binary mask of the tooth to identify the space changes. Different from the former research that focused on the variations of annotation based on panoramic images, this paper is trying to further improve the ability to segment panoramic radiographs by adding another

angle of oral radiographs to the training set which are called tangential images. Although many papers demonstrate good performance in segmenting out different structures of the oral image, few utilize them for further applications. An innovation of this paper is the utilization of a well-trained deep-learning model to predict tooth segmentation and suggest implant planning. For treatment of missing teeth, the dental implant has been considered as one of the common methods. Implant failure usually occurs due to the inaccurate choice of the implant location. Hence it is crucial to identify the correct location to ensure the success of the implant. In this application scenario, deep learning-based analytic tools can help to segment the tooth image and calculate the location of possible implants given dental panoramic images because the radiographic examination is a very common process for basic examination before any plan of treatment. Therefore, the second part of this paper focuses on implant planning after fine-tuning the best CNN model and using the prediction from the model and some other image-processing methods and machine-learning algorithms to help calculate the potential location, especially where the main direction of the implant is on the original x-ray images.

There are limitations to the application of the implant plan, as it requires at least two adjacent teeth around the missing area one on the left and one on the right. Also, it can only provide a single tooth implant suggestion based on the computation logic of the second part. When there are large missing areas that require more than one implant, such a method in the article is not useful. Future works will focus on how to expand the application scenarios of the current computation process to more common situations. Also, new deep learning architectures such as attention can be applied to the current network designs.

Despite the limitations of this study, a deep learning model is constructed using both panoramic and tangential images of patients' oral cavities to train a Convolutional Neural Network (CNN). The model predicts tooth images, offering suggestions for implant position prediction. This model shows acceptable results for the accuracy of predicting implant position, indicating its capability for clinical usage.

REFERENCES

- [1] Chen, Chen, T.-Y., Mao, Y.-C., Lin, S.-Y., Huang, Y.-Y., Chen, C.-A., Lin, Y.-J., Hsu, Y.-M., Li, C.-A., Chiang, W.-Y., Wong, K.-Y., & Abu, P. A. R. (2022). Automated Detection System Based on Convolution Neural Networks for Retained Root, Endodontic Treated Teeth, and Implant Recognition on Dental Panoramic Images. *IEEE Sensors Journal*, 22(23), 23293–23306. <https://doi.org/10.1109/JSEN.2022.3211981>
- [2] Chandrashekar, AlQarni, S., Bumann, E. E., & Lee, Y. (2022). Collaborative deep learning model for tooth segmentation and identification using panoramic radiographs. *Computers in Biology and Medicine*, 148, 105829–105829. <https://doi.org/10.1016/j.compbiomed.2022.105829>
- [3] Cui, Li, C., Chen, N., Wei, G., Chen, R., Zhou, Y., Shen, D., & Wang, W. (2021). TSegNet: An efficient and accurate tooth segmentation network on 3D dental model. *Medical Image Analysis*, 69, 101949–101949. <https://doi.org/10.1016/j.media.2020.101949>
- [4] Lee, Chung, M., Lee, M., & Shin, Y.-G. (2022). Tooth instance segmentation from cone-beam CT images through point-based detection and Gaussian disentanglement. *Multimedia Tools and Applications*, 81(13), 18327–18342. <https://doi.org/10.1007/s11042-022-12524-9>
- [5] Kohinata, Kitano, T., Nishiyama, W., Mori, M., Iida, Y., Fujita, H., & Katsumata, A. (2023). Deep learning for preliminary profiling of panoramic images. *Oral Radiology*, 39(2), 275–281. <https://doi.org/10.1007/s11282-022-00634-x>
- [6] Chang, H.J., Lee, S.J., Yong, T.H. et al. Deep Learning Hybrid Method to Automatically Diagnose Periodontal Bone Loss and Stage Periodontitis. *Sci Rep* 10, 7531 (2020). <https://doi.org/10.1038/s41598-020-64509-z>
- [7] Kohlakala, Coetzer, J., Bertels, J., & Vandermeulen, D. (2022). Deep learning-based dental implant recognition using synthetic X-ray images. *Medical & Biological Engineering & Computing*, 60(10), 2951–2968. <https://doi.org/10.1007/s11517-022-02642-9>
- [8] Zhao, Li, P., Gao, C., Liu, Y., Chen, Q., Yang, F., & Meng, D. (2020). TSASNet: Tooth segmentation on dental panoramic X-ray images by Two-Stage Attention Segmentation Network. *Knowledge-Based Systems*, 206, 106338. <https://doi.org/10.1016/j.knsys.2020.106338>
- [9] Silva, Pinheiro, L., Oliveira, L., & Pithon, M. (2020). A study on tooth segmentation and numbering using end-to-end deep neural networks. 2020 33rd SIBGRAPI Conference on Graphics, Patterns and Images (SIBGRAPI), 164–171. <https://doi.org/10.1109/SIBGRAPI51738.2020.00030>
- [10] Chen, Du, H., Yun, Z., Yang, S., Dai, Z., Zhong, L., Feng, Q., & Yang, W. (2020). Automatic Segmentation of Individual Tooth in Dental

CBCT Images From Tooth Surface Map by a Multi-Task FCN. IEEE Access, 8, 97296–97309. <https://doi.org/10.1109/ACCESS.2020.2991799>

- [11] Chen, Zhang, K., Lyu, P., Li, H., Zhang, L., Wu, J., & Lee, C.-H. (2019). A deep learning approach to automatic teeth detection and numbering based on object detection in dental periapical films. *Scientific Reports*, 9. <https://doi.org/10.1038/s41598-019-40414-y>
- [12] Khan, Talha, M., Khattak, A. S., & Qasim, M. (2013). Realization of Balanced Contrast Limited Adaptive Histogram Equalization (BCLAHE) for Adaptive Dynamic Range Compression of real time medical images. *Proceedings of 2013 10th International Bhurban Conference on Applied Sciences & Technology (IBCAST)*, 117–121. <https://doi.org/10.1109/IBCAST.2013.6512142>
- [13] Huang, Lin, L., Tong, R., Hu, H., Zhang, Q., Iwamoto, Y., Han, X., Chen, Y.-W., & Wu, J. (2020). UNet 3+: A Full- Scale Connected UNet for Medical Image Segmentation. *ICASSP 2020 - 2020 IEEE International Conference on Acoustics, Speech and Signal Processing (ICASSP)*, 1055–1059. <https://doi.org/10.1109/ICASSP40776.2020.9053405>
- [14] Silva, Oliveira, L., & Pithon, M. (2018). Automatic segmenting teeth in X-ray images: Trends, a novel data set, benchmarking and future perspectives. *Expert Systems with Applications*, 107, 15–31. <https://doi.org/10.1016/j.eswa.2018.04.001>
- [15] Isensee, Jaeger, P. F., Kohl, S. A. A., Petersen, J., & Maier-Hein, K. H. (2021). nnU-Net: a self-configuring method for deep learning-based biomedical image segmentation. *Nature Methods*, 18(2), 203–211. <https://doi.org/10.1038/s41592-020-01008-z>
- [16] Ma, Chen, J., Ng, M., Huang, R., Li, Y., Li, C., Yang, X., & Martel, A. L. (2021). Loss odyssey in medical image segmentation. *Medical Image Analysis*, 71, 102035–102035. <https://doi.org/10.1016/j.media.2021.102035>
- [17] A Novel Collaborative Learning Model for Teeth and Fillings in Radiographs. (2023). In *Health & Medicine Week* (p. 1013). NewsRX LLC.
- [18] Putra, Doi, C., Yoda, N., Astuti, E. R., & Sasaki, K. (2022). Current applications and development of artificial intelligence for digital dental radiography. *Dento-Maxillo-Facial Radiology*, 51(1), 20210197–20210197. <https://doi.org/10.1259/dmfr.20210197>
- [19] Park, J., Lee, J., Moon, S., & Lee, K. (2022). Deep Learning Based Detection of Missing Tooth Regions for Dental Implant Planning in Panoramic Radiographic Images. *Applied Sciences*, 12(3), 1595-. <https://doi.org/10.3390/app12031595>
- [20] Lee, S., Woo, S., Yu, J., Seo, J., Lee, J., & Lee, C. (2020). Automated CNN-Based Tooth Segmentation in Cone-Beam CT for Dental Implant Planning. *IEEE Access*, 8, 50507–50518. <https://doi.org/10.1109/ACCESS.2020.2975826>
- [21] R. Bodhe, S. Sivakumar and A. Raghuvanshi, "Design and Development of Deep Learning Approach for Dental Implant Planning," 2022 International Conference on Green Energy, Computing and Sustainable Technology (GECOST), Miri Sarawak, Malaysia, 2022, pp. 269-274, doi: 10.1109/GECOST55694.2022.10010527.
- [22] Kurt Bayrakdar, S., Orhan, K., Bayrakdar, I. S., Bilgir, E., Ezhov, M., Gusarev, M., & Shumilov, E. (2021). A deep learning approach for dental implant planning in cone-beam computed tomography images. *BMC Medical Imaging*, 21(1), 86–86. <https://doi.org/10.1186/s12880-021-00618-z>

Please fill in the all authors’ background:

Position can be chosen from:				
Prof. / Assoc. Prof. / Asst. Prof. / Lecture / Dr. / Ph. D Candidate / Postgraduate, etc.				
Full Name	Email Address	Position	Research Interests	Personal Website (if any)
Yang Xing	yangx9@bu.edu	Postgraduate	Computer Vision	
Peixi Liao	liaopx@bu.edu	Prof.	Dentistry	
Reem AwdhE Alasleh	alsalehr@bu.edu	Dr.	Dentistry	
Vissuta Khampatee	vissutak@bu.edu	Dr.	Dentistry	
Farshid Alizadeh-Shabdiz	alizadeh@bu.edu	Prof.	Computer Vision	